



Effect of the Biofield Energy Healing Treatment on Physicochemical and Thermal Properties of Vitamin D₃ (Cholecalciferol)



Alice Branton¹, Mahendra Kumar Trivedi¹, Dahryn Trivedi¹, Gopal Nayak¹ and Snehasis Jana^{2*}

¹Trivedi Global, USA

²Trivedi Science Research Laboratory Pvt Ltd., India

*Corresponding author: Snehasis Jana, Trivedi Science Research Laboratory Pvt Ltd, Bhopal, India, Tel: +91- 022-25811234, Email: publication@trivedieffect.com

Submission: 📅: September 05, 2018; Published: 📅: September 20, 2018

Abstract

Vitamin D₃ (cholecalciferol) is a fat-soluble vitamin, which increases the intestinal absorption of minerals (i.e., calcium, magnesium, etc.) and also helps in the prevention and treatment of vitamin D deficiency diseases like rickets, osteoporosis, etc. This research was designed to evaluate the impact of the Trivedi Effect[®]-Consciousness Energy Healing Treatment on the physicochemical and thermal properties of cholecalciferol using the modern analytical technique. The cholecalciferol sample was divided into two parts. One part of the sample was considered as the control sample, while the other portion was subjected to the Biofield Treatment remotely by a renowned Biofield Energy Healer, Alice Branton and was termed as the treated sample. The powder XRD peak intensities and crystallite sizes were significantly altered ranging from -71.04% to 85.29% and -58.83% to 712.16% respectively, whereas, the average crystallite size was significantly increased by 6.81% in the treated sample compared to the control sample. The particle size values were significantly decreased by 76.95% (d₁₀), 40.84% (d₅₀), 17.44% (d₉₀), and 34.30% [D (4,3)], thus, significantly increased the surface area by 152.23% in the treated sample compared to the control sample. The latent heat of fusion and the maximum thermal degradation temperature were increased by 5.60% and 8.5%, respectively in the treated sample compared to the control sample. The total weight loss was increased by 4.76%; however, the residue amount was significantly decreased by 75.1% in the treated sample compared with the control sample. The Biofield Energy Healing Treatment generates a new polymorphic form of cholecalciferol which might offer better solubility, absorption, bioavailability, and thermal stability. The Biofield Energy Treated cholecalciferol would be more efficacious in the nutraceutical/pharmaceutical formulations for the better therapeutic responses against rickets, osteoporosis, cardiovascular diseases, cancer, diabetes, etc. It can also help to enhance the intestinal absorption of minerals like calcium, zinc, magnesium, iron, and phosphate.

Keywords: Cholecalciferol; The trivedi effect[®]; Consciousness energy healing treatment; PXRD; Particle size; Surface area; DSC; TGA/DTG

Introduction

Vitamin D₃ (cholecalciferol) is a fat-soluble vitamin responsible for the increasing intestinal absorption of several vital minerals like calcium, zinc, magnesium, iron, and phosphate and other biological activity in the body [1]. Naturally, it is produced in the body from 7-dehydrocholesterol by means of photochemical reaction under the skin with the help of solar energy. It can also be available from the foods (cod liver oil, milk, fatty fish like salmon, tuna, etc.) or nutraceutical/pharmaceutical supplements. It plays a vital role in maintaining the immunity, skeletal, cardiovascular, and reproductive systems [2,3]. Vitamin D₃ plays a vital role for the prevention and treatment of several diseases like rickets, osteoporosis, cardiovascular diseases, cancer, diabetes mellitus, mental disorders, multiple sclerosis, infections, etc. [4-6]. Nowadays vitamin D₃ deficiency is pandemic, mostly under-diagnosed and under-treated nutritional deficiency all over the world. Cholecalciferol can be used as a food and dietary supplement for the prevention and treatment

of vitamin D₃ deficiency disease [7]. Cholecalciferol is hydroxylated at position C-25 to convert 25-hydroxycholecalciferol (also known as calcidiol), which is more stable in blood. Consequently, the second hydroxylation occurs at position C1 α to produce its biologically active form -1,25-dihydroxycholecalciferol (known as calcitriol) [5-7]. Vitamin D₃ toxicity can be resultant with the high dose of supplementation, which leads to hypercalcemia, polyuria, polydipsia, weakness, insomnia, and mental retardation [1]. Chemically vitamin D₃ contains three double bonds in its structure, which are usually responsible for the cis and trans structural conformation. The factors that directly affect the vitamin D₃ bioavailability are insoluble in water, dietary fiber, genetic factors, and vitamin D₃ status [8,9]. It is very sensitive to the light and air [10,11]. Thus, stability, solubility, and bioavailability of vitamin D₃ are the major concerned.

All over the world, scientists are doing research for the improvement of dissolution, absorption, and bioavailability of the pharmaceutical grade and/or nutraceutical form of vitamin D₃, because it has poor absorption and bioavailability in the body [12]. The Trivedi Effect®-Consciousness Energy Healing Treatment has shown a significant effect on various physicochemical properties such as particle size, surface area, thermal behaviour, and bioavailability profile of pharmaceutical and nutraceutical compounds [13-15]. The Trivedi Effect® is natural and the only scientifically proven phenomenon in which a person can harness this inherently intelligent energy from the Universe and transmit it anywhere on the planet through the mediation of neutrinos [16]. There is an infinite and para-dimensional unique electromagnetic field exists surrounding the body of every living organism called the "Biofield". The Biofield based Energy Therapies have been reported with significantly beneficial outcomes against various disease conditions [17]. The National Institute of Health/National Center for Complementary and Alternative Medicine (NIH/NCCAM) recommend and included the Energy therapy under the Complementary and Alternative Medicine (CAM) category along with Ayurvedic medicine, naturopathy, essential oils, traditional Chinese herbs and medicines, homeopathy, Tai Chi, Qi Gong, yoga, meditation, deep breathing, special diets, massage, acupuncture, acupressure, progressive relaxation, relaxation techniques, guided imagery, healing touch, Reiki, movement therapy, chiropractic/osteopathic manipulation, hypnotherapy, pilates, Roling structural integration, mindfulness, cranial sacral therapy, aromatherapy, and applied prayer. The CAM has been accepted by the most of the U.S. population because of several advantages [18,19]. In this aspect, the Trivedi Effect®-Consciousness Energy Healing Treatment (Biofield Energy Treatment) has a significant impact for the transformation of various properties of the object(s), and the outcomes were published in numerous peer-reviewed scientific journals. The Biofield Energy Treatment has the unprecedented capability to alter the physicochemical, structural, and behavioural properties of metals and ceramics [20-22], organic compounds [23,24], nutraceuticals [25,26], pharmaceuticals [27,28], microorganisms [29,30], various living cells [31,32], and to improve the overall productivity of crops [33,34]. The current study was designed and evaluated the impact of the Trivedi Effect®-Consciousness Energy Healing Treatment on the physicochemical, thermal, and behavioural properties of cholecalciferol using powder X-ray diffraction (PXRD), particle size analysis (PSA), differential scanning calorimetry (DSC), and thermogravimetric analysis (TGA)/ differential thermogravimetric analysis (DTG).

Materials and Methods

Chemicals and reagents

The cholecalciferol (>98%) was purchased from Sigma-Aldrich, India. All other chemicals used during the experiments were of analytical grade available in India.

Consciousness energy healing treatment strategies

The test sample (cholecalciferol) was divided into two equal parts. One part of the test sample was treated with the Trivedi

Effect®-Consciousness Energy Healing Treatment remotely under standard laboratory conditions for 3 minutes, known as the Trivedi Effect® Treated or Biofield Energy Treated cholecalciferol sample. This Biofield Energy Treatment was provided through the healer's unique energy transmission process by the renowned Biofield Energy Healer, Alice Branton, USA, to one part of the cholecalciferol sample. However, the second part of cholecalciferol was considered as the control sample (no Biofield Energy Treatment was provided). Further, the control sample was treated with a "sham" healer for the comparison purpose. The "sham" healer did not have any knowledge about the Biofield Energy Treatment. After treatment, the Biofield Energy Treated and untreated samples were kept in sealed conditions and characterized using PXRD, PSA, DSC, and TGA/DTG techniques.

Characterization

Powder X-ray Diffraction (PXRD) Analysis

The PXRD analysis of cholecalciferol was performed with the help of Rigaku MiniFlex-II Desktop X-ray diffractometer (Japan) [35,36]. The Cu K α radiation source tube output voltage used was 30 kV, and tube output current was 15 mA. Scans were performed at room temperature. The average size of individual crystallites was calculated from PXRD data using the Scherrer's formula (1)

$$G = \frac{k\lambda}{\beta \cos\theta} \quad (1)$$

Where k is the equipment constant (0.94), G is the crystallite size in nm, λ is the radiation wavelength (0.154056 nm for K α 1 emission), β is the full-width at half maximum (FWHM), and θ is the Bragg angle [37]. The percent change in crystallite size (G) of cholecalciferol was calculated using the following equation 2:

$$\% \text{ change in crystallite size} = \frac{[G_{\text{Treated}} - G_{\text{control}}]}{G_{\text{control}}} \times 100 \quad (2)$$

Where G_{Control} and G_{Treated} are the crystallite size of the control and the Biofield Energy Treated samples, respectively.

Particle size analysis (PSA)

The particle size analysis of cholecalciferol was conducted on Malvern Mastersizer 2000, from the UK with a detection range between 0.01 μm to 3000 μm using wet method [38,39]. The sample unit (Hydro MV) was filled with a dispersant medium (sunflower oil) and the stirrer operated at 2500rpm. The PSA analysis of cholecalciferol was performed to obtain the average particle size distribution. Where d (0.1) μm , d (0.5) μm , d (0.9) μm represent particle diameter corresponding to 10%, 50% and 90%, respectively of the cumulative distribution. D(4,3) represents the average mass-volume diameter, and SSA is the specific surface area (m^2/g). The calculations were done by using software Mastersizer Ver. 5.54.

The percent change in particle sizes (d) for cholecalciferol at below 10% level (d_{10}), 50% level (d_{50}), 90% level (d_{90}), and D (4,3) was calculated using the following equation 3:

$$\% \text{ change in particle size} = \frac{[d_{\text{Treated}} - d_{\text{control}}]}{d_{\text{control}}} \times 100 \quad (3)$$

Where $d_{Control}$ and $d_{Treated}$ are the particle size (μm) for at below 10% level (d_{10}), 50% level (d_{50}), and 90% level (d_{90}) of the control and the Biofield Energy Treated samples, respectively.

The percent change in surface area (S) was calculated using the following equation 4:

$$\% \text{ change in surface area} = \frac{[S_{Treated} - S_{Control}]}{S_{Control}} \times 100 \quad (4)$$

Where $S_{Control}$ and $S_{Treated}$ are the surface area of the control and the Biofield Energy Treated cholecalciferol, respectively.

Differential scanning calorimetry (DSC)

The DSC analysis of cholecalciferol was performed with the help of DSC Q200, TA instruments. The sample of ~1 mg was loaded to the aluminium sample pan at a heating rate of 10 °C/min from 30 °C to 350 °C [38,39]. The % change in melting point (T) was calculated using the following equation 5:

$$\% \text{ change in melting point} = \frac{[T_{Treated} - T_{Control}]}{T_{Control}} \times 100 \quad (5)$$

Where $T_{Control}$ and $T_{Treated}$ are the melting point of the control and treated samples, respectively.

The percent change in the latent heat of fusion (ΔH) was calculated using the following equation 6:

$$\% \text{ Change in latent heat of fusion} = \frac{[\Delta H_{Treated} - \Delta H_{Control}]}{\Delta H_{Control}} \times 100 \quad (6)$$

Where $\Delta H_{Control}$ and $\Delta H_{Treated}$ are the latent heat of fusion of the control and treated cholecalciferol, respectively.

Thermal gravimetric analysis (TGA) / Differential thermogravimetric analysis (DTG)

TGA/DTG thermograms of cholecalciferol were obtained with the help of TGA Q50 TA instruments. A sample of ~2-8 mg was loaded to the platinum crucible at a heating rate of 10°C/min/min from 25°C to 1000°C with the recent literature [38-39]. The % change in weight loss (W) was calculated using the following

equation 7:

$$\% \text{ change in weight loss} = \frac{[W_{Treated} - W_{Control}]}{W_{Control}} \times 100 \quad (7)$$

Where $W_{Control}$ and $W_{Treated}$ are the weight loss of the control and the Biofield Energy Treated cholecalciferol, respectively.

The % change in maximum thermal degradation temperature (T_{max}) (M) was calculated using the following equation 8:

$$\% \text{ Change in Tmax (M)} = \frac{[M_{Treated} - M_{Control}]}{M_{Control}} \times 100 \quad (8)$$

Where $M_{Control}$ and $M_{Treated}$ are the T_{max} values of the control and the Biofield Energy Treated cholecalciferol, respectively.

Results and Discussion

Powder X-ray diffraction (PXRD) analysis

The PXRD diffractogram of the control cholecalciferol showed sharp and intense peaks at Bragg's angle (2θ) equal to 4.05°, 5.15°, 6.69°, 8.62°, 9.84°, 12.94°, 13.52°, 15.39°, 15.64°, 18°, 18.24°, 21.79°, 23.52°, 23.82°, 24.85°, and 30° (Figure 1). Similarly, the Biofield Energy Treated sample showed sharp and intense peaks at Bragg's angle (2θ) equal to 5.32°, 5.44°, 6.78°, 8.79°, 9.45°, 13.12°, 13.91°, 15.72°, 15.92°, 18.1°, 18.13°, 21.8°, 23.35°, 23.89°, 25.21°, and 29.95° (Figure 1). The sharp and intense peaks in the chromatograms indicating that both the samples were crystalline. The control and the Biofield Energy Treated cholecalciferol samples showed the highest peak intensity at 2θ equal to 18.24° and 18.24°, respectively (Table 1, entry 11). The peak intensities of the Biofield Energy Treated cholecalciferol were significantly altered ranging from -71.04% to 85.29% compared to the control sample. Similarly, the crystallite sizes of the Biofield Energy Treated cholecalciferol sample were significantly altered ranging from -58.83% to 712.16% compared to the control sample. Overall, the average crystallite size of the Biofield Energy Treated cholecalciferol (288.13nm) was significantly increased by 6.81% compared with the control sample (269.75nm).

Table 1: PXRD data for the control and the Biofield Energy Treated cholecalciferol.

| Entry No. | Bragg Angle (°2 θ) | | Peak Intensity (%) | | | Crystallite Size (G, nm) | | |
|-----------|----------------------------|---------|--------------------|---------|-----------------------|--------------------------|---------|-----------------------|
| | Control | Treated | Control | Treated | % Change ^a | Control | Treated | % Change ^b |
| 1 | 4.85 | 5.32 | 1408 | 1270 | -9.8 | 192 | 176 | -8.33 |
| 2 | 5.15 | 5.44 | 281 | 139 | -50.53 | 1030 | 612 | -40.58 |
| 3 | 6.69 | 6.78 | 224 | 220 | -1.79 | 238 | 196 | -17.65 |
| 4 | 8.62 | 8.79 | 318 | 305 | -4.09 | 180 | 139 | -22.78 |
| 5 | 9.84 | 9.45 | 183 | 53 | -71.04 | 54 | 358 | 562.96 |
| 6 | 12.94 | 13.12 | 494 | 899 | 81.98 | 87 | 48 | -44.83 |
| 7 | 13.52 | 13.91 | 247 | 116 | -53.04 | 244 | 239 | -2.05 |
| 8 | 15.39 | 15.72 | 1538 | 1510 | -1.82 | 137 | 124 | -9.49 |
| 9 | 15.64 | 15.92 | 941 | 264 | -71.94 | 131 | 428 | 226.72 |
| 10 | 18 | 18.1 | 1881 | 1447 | -23.07 | 314 | 230 | -26.75 |
| 11 | 18.24 | 18.13 | 2307 | 1545 | -33.03 | 532 | 219 | -58.83 |
| 12 | 21.79 | 21.8 | 546 | 776 | 42.12 | 171 | 149 | -12.87 |

| | | | | | | | | |
|----|--------------------------|-------|-----|-----|-------|--------|--------|--------|
| 13 | 23.52 | 23.35 | 626 | 482 | -23 | 93 | 168 | 80.65 |
| 14 | 23.82 | 23.89 | 102 | 188 | 84.31 | 733 | 781 | 6.55 |
| 15 | 24.85 | 25.21 | 222 | 200 | -9.91 | 106 | 142 | 33.96 |
| 16 | 30 | 29.95 | 34 | 63 | 85.29 | 74 | 601 | 712.16 |
| 17 | Average crystallite size | | | | | 269.75 | 288.13 | 6.81 |

^adenotes the percentage change in the peak intensity of the Biofield Energy Treated sample with respect to the control sample, ^bdenotes the percentage change in the crystallite size of the Biofield Energy Treated sample with respect to the control sample.

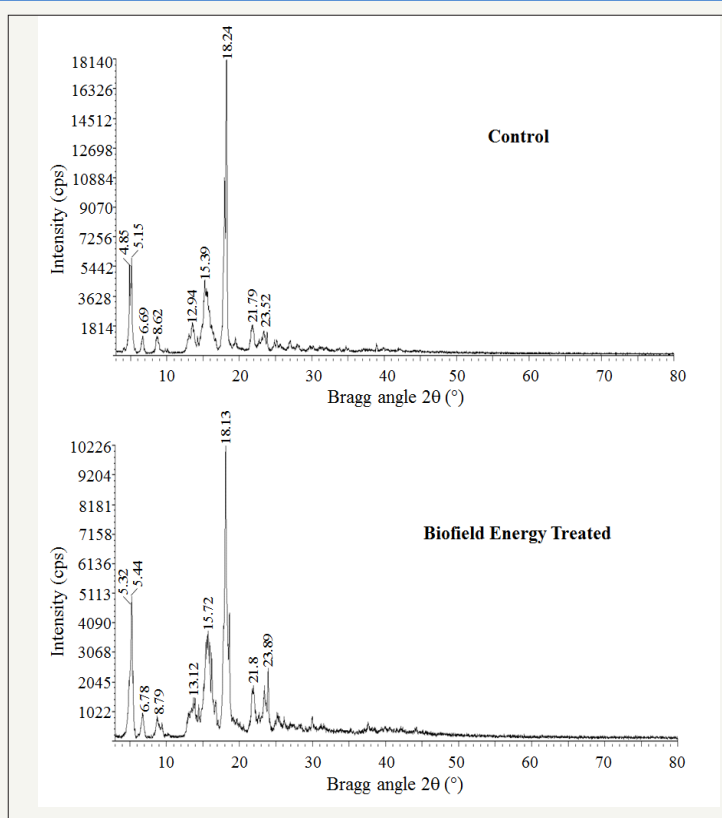


Figure 1: PXRD diffractograms of the control and the Biofield Energy Treated cholecalciferol.

Significant variations that were experimentally observed in the crystallite sizes and peak intensities indicated the modification of the crystal morphology of the Biofield Energy Treated cholecalciferol compared to the control sample. The literature says that if any change in the peak intensity of the diffraction face on the crystalline compound changes the crystal morphology [40]. The alterations in the PXRD pattern provide proof of polymorphic transitions [41,42]. The Trivedi Effect[®]-Consciousness Energy Healing Treatment probably produced a new polymorphic form of cholecalciferol through the Biofield Energy via neutrino oscillations [16]. The drug performance of the pharmaceuticals, such as bioavailability, therapeutic efficacy, and toxicity, because of their thermodynamic and physicochemical properties like melting point, energy, stability, and especially solubility, are different (probably the improvement) from the original form due to different polymorphic forms [43,44]. Thus, the Trivedi Effect[®] Treated cholecalciferol would be a better option for designing of more effective pharmaceutical formulations.

Particle size analysis (PSA)

The PSD analysis of both the control and the Biofield Energy Treated cholecalciferol were performed, and the data are compared and presented in Table 2. The particle size values of the control cholecalciferol at d_{10} , d_{50} , d_{90} , and $D(4,3)$ were 190.17 μm , 447.09 μm , 765.36 μm , and 463.38 μm , respectively. Similarly, the particle sizes of the Biofield Energy Treated cholecalciferol at d_{10} , d_{50} , d_{90} , and $D(4,3)$ were 43.84 μm , 264.51 μm , 631.86 μm , and 304.46 μm , respectively. The particle size values in the Biofield Energy Treated cholecalciferol were significantly decreased at d_{10} , d_{50} , d_{90} , and $D(4,3)$ by 76.95%, 40.84%, 17.44%, and 34.30%, respectively compared with the control sample. The specific surface area of the Biofield Energy Treated cholecalciferol (0.0734 m^2/g) was significantly increased by 152.23% compared to the control sample (0.0291 m^2/g). The reason behind decreased particle size assumed to be the impact of the Trivedi Effect[®]-Consciousness Energy Healing Treatment. The Biofield Energy Treatment might be acting as an

external force for breaking the larger particles to smaller particles in size of cholecalciferol sample; thus, increasing the surface area. It was reported that the particle size, shape, and surface area impact the solubility, dissolution rate, absorption, bioavailability, and even the therapeutic efficacy of a drug substance [45,46]. Vitamin D₃ is

lipophilic in nature and poor solubility profile in water responsible for the poor bioavailability of vitamin D₃ status [8,9]. Thus, it can be assumed that the Biofield Energy Treated cholecalciferol would enhance the solubility, absorption, and therapeutic efficacy when used in the nutraceutical/pharmaceutical formulations.

Table 2: Particle size distribution of the control and the Biofield Energy Treated cholecalciferol.

| Parameter | d ₁₀ (µm) | d ₅₀ (µm) | d ₉₀ (µm) | D (4,3) (µm) | SSA (m ² /g) |
|--------------------|----------------------|----------------------|----------------------|--------------|-------------------------|
| Control | 190.17 | 447.09 | 765.36 | 463.38 | 0.0291 |
| Biofield Treated | 43.84 | 264.51 | 631.86 | 304.46 | 0.0734 |
| Percent change*(%) | -76.95 | -40.84 | -17.44 | -34.3 | 152.23 |

d₁₀, d₅₀, and d₉₀: particle diameter corresponding to 10%, 50%, and 90% of the cumulative distribution, D (4,3): the average mass-volume diameter, and SSA: the specific surface area.

*denotes the percentage change in the particle size distribution of the Biofield Energy Treated sample with respect to the control sample

Differential scanning calorimetry (DSC) analysis

DSC thermograms of both control and the Biofield Energy Treated cholecalciferol are presented in Figure 2. The control and Biofield Energy Treated cholecalciferol showed sharp endothermic peaks at 87.81°C and 88.25°C, respectively in the thermograms (Figure 2). The experimental results closely match to the literature reported data [47]. Similarly, the latent heat of fusion (ΔH_{fusion}) of the control and the Biofield Energy Treated cholecalciferol were 57.81 J/g and 61.05, respectively (Table 3). The melting point and

ΔH_{fusion} of the Biofield Energy Treated sample were increased by 0.5% and 5.60%, respectively compared to the control sample. The literature says that any change in the latent heat of fusion can be attributed to the disrupted molecular chains and the crystal structure [48]. Therefore, it can be assumed that the Trivedi Effect®-Consciousness Energy Healing Treatment might be responsible for the disruption the molecular chains and crystal structure of cholecalciferol which improved the thermal stability of the treated sample compared with the control sample.

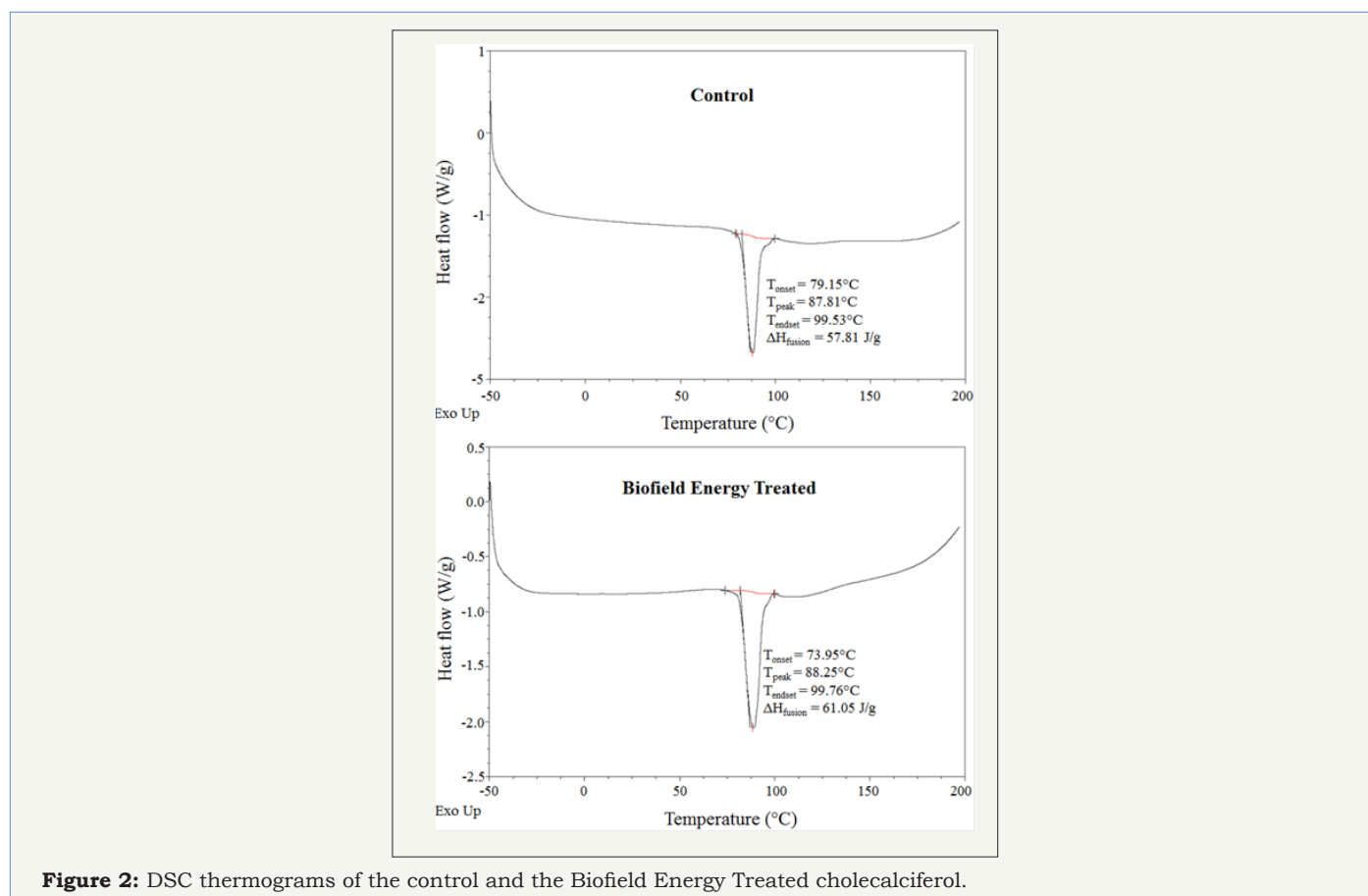


Figure 2: DSC thermograms of the control and the Biofield Energy Treated cholecalciferol.

Table 3: DSC data for both control and Biofield Energy Treated samples of cholecalciferol.

| Sample | Melting Temp (°C) | ΔH_{fusion} (J/g) |
|-------------------------|-------------------|----------------------------------|
| Control Sample | 87.81 | 57.81 |
| Biofield Energy Treated | 88.25 | 61.05 |
| % Change* | 0.5 | 5.6 |

ΔH_{fusion} : Latent heat of fusion.

*denotes the percentage change of the Biofield Energy Treated cholecalciferol with respect to the control sample

Thermal gravimetric analysis (TGA) / Differential thermogravimetric analysis (DTG)

The TGA thermograms of the control and the Biofield Energy Treated cholecalciferol samples showed one step of thermal degradation (Figure 3). The Biofield Energy Treated cholecalciferol

showed a total weight loss of 4.76% more compared to the control sample (Table 4). Therefore, the residue amount was significantly decreased by 75.1% in the Biofield Energy Treated cholecalciferol compared to the control sample (Table 4).

Table 4: TGA/DTG data of the control and Biofield Energy Treated samples of cholecalciferol.

| Sample | TGA | | DTG |
|-------------------------|-----------------------|-----------|-----------------------|
| | Total Weight Loss (%) | Residue % | T_{max} (°C) |
| Control | 94.035 | 5.965 | 263.79 |
| Biofield Energy Treated | 98.515 | 1.485 | 286.2 |
| % Change* | 4.76 | -75.1 | 8.5 |

T_{max} : The temperature at which maximum weight loss takes place in TG or peak temperature in DTG.

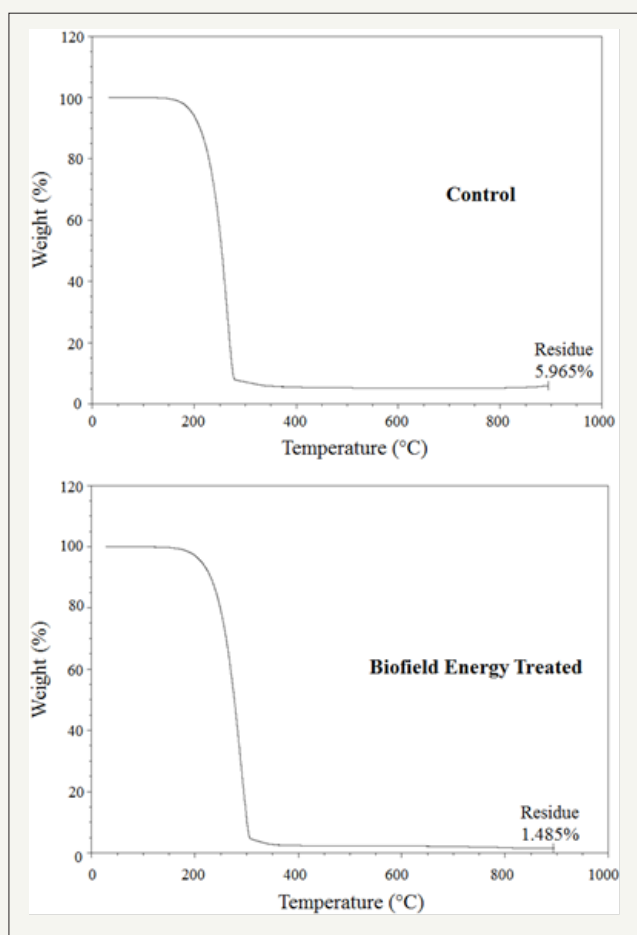


Figure 3: TGA thermograms of the control and the Biofield Energy Treated cholecalciferol.

denotes the percentage change of the Biofield Energy Treated sample with respect to the control sample,

The DTG of the control and the Biofield Energy Treated cholecalciferol also showed one peak in the thermograms (Figure

4). The T_{max} of the Biofield Energy Treated sample was significantly increased by 8.5% compared to the control sample (Table 4). Overall, TGA/DTG analysis of cholecalciferol samples revealed that the thermal stability of the Biofield Energy Treated sample was altered compared with the control sample.

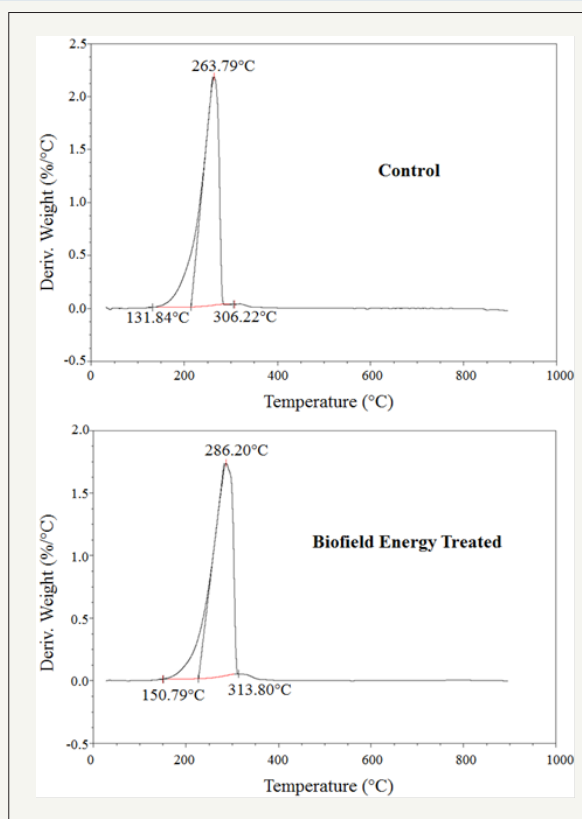


Figure 4: DTG thermograms of the control and the Biofield Energy Treated cholecalciferol.

Conclusion

The experimental results suggest that the Trivedi Effect®-Consciousness Energy Healing Treatment has a significant effect on the particle size, surface area, and thermal properties of vitamin D₃ (cholecalciferol). The PXRD data indicated that the peak intensities of the Biofield Energy Treated cholecalciferol were significantly altered ranging from -71.04% to 85.29% compared to the control sample. Similarly, the crystallite sizes of the Biofield Energy Treated cholecalciferol were significantly altered ranging from -58.83% to 712.16% compared to the control sample. The average crystallite size of the Biofield Energy Treated cholecalciferol was significantly increased by 6.81% compared with the control sample. The particle size values in the Biofield Energy Treated cholecalciferol were significantly decreased at d_{10} , d_{50} , d_{90} , and $D(4,3)$ by 76.95%, 40.84%, 17.44%, and 34.30%, respectively compared to the control sample. Therefore, the specific surface area of the Biofield Energy Treated cholecalciferol was significantly increased by 152.23% compared to the control sample. The melting point and ΔH_{fusion} of the Biofield Energy Treated sample were increased by 0.5% and 5.60%, respectively compared to the control sample. However, the total weight loss was increased by 4.76%; however, the residue amount was significantly decreased by 75.1% in the Biofield Energy Treated sample compared with the control sample. The T_{max} was significantly increased by 8.5% in the Biofield Energy Treated cholecalciferol compared with the control sample. The Trivedi Effect®-Consciousness Energy Healing Treatment lead to

the generation of a new polymorphic form of cholecalciferol which might offer better solubility, dissolution, absorption, bioavailability and thermal stability compared with the control sample. Therefore, the Trivedi Effect®-Consciousness Energy Healing Treated cholecalciferol would be more beneficial to maintain the overall quality of life; maintain the immunity, skeletal, cardiovascular, and reproductive systems; increase the intestinal absorption of several vital minerals like calcium, zinc, magnesium, iron, and phosphate in the body. Similarly, the treated cholecalciferol would be more efficacious in the pharmaceutical formulations that might offer better therapeutic responses against rickets, osteoporosis, cardiovascular diseases, cancer, diabetes mellitus, mental disorders, multiple sclerosis, infections, etc.

Acknowledgement

The authors are grateful to Central Leather Research Institute, SIPRA Lab Ltd, Trivedi Science, Trivedi Global, Inc., Trivedi Testimonials, and Trivedi Master Wellness for their assistance and support during this work.

Conflict of Interest

Authors declare no conflict of interest.

References

1. https://en.wikipedia.org/wiki/Vitamin_D
2. Zhang R, Naughton DP (2010) Vitamin D in health and disease: Current perspectives. *Nutr J* 9: 65.

3. Gouni Berthold I, Krone W, Berthold HK (2009) Vitamin D and cardiovascular disease. *Curr Vasc Pharmacol* 7(3): 414-422.
4. Simana E, Simian R, Portnoy S, Jaffe A, Dekel BZ (2015) Feasibility study -Vitamin D loading determination by FTIR-ATR. *Information & Control Systems* 76: 107-111.
5. Ritu G, Gupta A (2014) Vitamin D deficiency in India: Prevalence, causalities and interventions. *nutrients* 6(2): 729-775.
6. Lawson DE, Wilson PW, Kodicek E (1969) Metabolism of vitamin D. A new cholecalciferol metabolite, involving loss of hydrogen at C-1, in chick intestinal nuclei. *Biochem J* 115(2): 269-277.
7. Mattila P, Lehtikoinen K, Kiiskinen T, Piironen V (1999) Cholecalciferol and 25-hydroxycholecalciferol content of chicken egg yolk as affected by the cholecalciferol content of feed. *J Agric Food Chem* 47(10): 4089-4092.
8. Lehmann U, Hirche F, Stangl GI, Hinz K, Westphal S, et al. (2013) Bioavailability of vitamin D(2) and D(3) in healthy volunteers, a randomized placebo-controlled trial. *J Clin Endocrinol Metab* 98(11): 4339-4345.
9. Borel P, Caillaud D, Cano NJ (2015) Vitamin D bioavailability: State of the art. *Crit Rev Food Sci Nutr* 55(9): 1193-1205.
10. Koshy KT, Beyer WF (1984) Vitamin D₃ (Cholecalciferol) in analytical profiles of drug substances. In: Florey K (Ed.), Vol 13, Academic Press, Inc, Orlando, USA, pp: 656-707.
11. Collins ED, Norman AW (2001) Vitamin D in Handbook of Vitamins, (3rd edn). In: Rucker RB, Suttie JW, McCormick DB, Machlin LJ, Marcel D (Eds.), Inc, New York, USA, pp. 51-114.
12. Chereson R (2009) Bioavailability, bioequivalence, and drug selection. In: Makoid CM, Vuchetich PJ, Banakar UV (Eds) Basic pharmacokinetics (1st edn) Pharmaceutical Press, London.
13. Trivedi MK, Branton A, Trivedi D, Shettigar H, Bairwa K, et al. (2015) Fourier transform infrared and ultraviolet-visible spectroscopic characterization of biofield treated salicylic acid and sparfloxacin. *Nat Prod Chem Res* 3: 186.
14. Trivedi MK, Patil S, Shettigar H, Singh R, Jana S (2015) An impact of biofield treatment on spectroscopic characterization of pharmaceutical compounds. *Mod Chem Appl* 3: 159.
15. Branton A, Jana S (2017) The influence of energy of consciousness healing treatment on low bioavailable resveratrol in male *Sprague Dawley* rats. *International Journal of Clinical and Developmental Anatomy* 3(3): 9-15.
16. Trivedi MK, Mohan TRR (2016) Biofield energy signals, energy transmission and neutrinos. *American Journal of Modern Physics* 5(6): 172-176.
17. Rubik B, Muehsam D, Hammerschlag R, Jain S (2015) Biofield science and healing: history, terminology, and concepts. *Glob Adv Health Med* 4: 8-14.
18. Barnes PM, Bloom B, Nahin RL (2008) Complementary and alternative medicine use among adults and children: United States, 2007. *Natl Health Stat Report* 12: 1-23.
19. Koithan M (2009) Introducing complementary and alternative therapies. *J Nurse Pract* 5(1): 18-20.
20. Trivedi MK, Patil S, Tallapragada RM Effect of biofield treatment on the physical and thermal characteristics of Silicon, Tin and Lead powders. *J Material Sci Eng* 2: 125.
21. Trivedi MK, Patil S, Tallapragada RM (2013) Effect of bio field treatment on the physical and thermal characteristics of vanadium pentoxide powders. *J Material Sci Eng* S11: 001.
22. Trivedi MK, Nayak G, Patil S, Tallapragada RM, Latiyal O (2015) Studies of the atomic and crystalline characteristics of ceramic oxide nano powders after bio field treatment. *Ind Eng Manage* 4: 161.
23. Trivedi MK, Branton A, Trivedi D, Nayak G, Panda P, et al. (2016) Isotopic abundance ratio analysis of 1,2,3-trimethoxybenzene (TMB) after biofield energy treatment (The Trivedi Effect®) using gas chromatography-mass spectrometry. *American Journal of Applied Chemistry* 4(4): 132-140.
24. Trivedi MK, Branton A, Trivedi D, Nayak G, Sethi KK, et al. (2016) Evaluation of isotopic abundance ratio in biofield energy treated nitrophenol derivatives using gas chromatography-mass spectrometry. *American Journal of Chemical Engineering* 4: 68-77.
25. Trivedi MK, Tallapragada RM, Branton A, Trivedi D, Nayak G, et al. (2015) Evaluation of biofield energy treatment on physical and thermal characteristics of selenium powder. *Journal of Food and Nutrition Sciences* 3: 223-228.
26. Trivedi MK, Tallapragada RM, Branton A, Trivedi D, Nayak G, et al. (2015) Physicochemical characterization of biofield energy treated calcium carbonate powder. *American Journal of Health Research* 3(6): 368-375.
27. Branton A, Jana S (2017) Effect of the biofield energy healing treatment on the pharmacokinetics of 25-hydroxyvitamin D₃ [25(OH)D₃] in rats after a single oral dose of vitamin D₃. *American Journal of Pharmacology and Phytotherapy* 2(1): 11-18.
28. Trivedi MK, Patil S, Shettigar H, Bairwa K, Jana S (2015) Spectroscopic characterization of chloramphenicol and tetracycline: An impact of biofield. *Pharm Anal Acta* 6: 395.
29. Trivedi MK, Branton A, Trivedi D, Gangwar M, Jana S (2015) Antimicrobial susceptibility, biochemical characterization and molecular typing of biofield treated *Klebsiella pneumoniae*. *J Health Med Inform* 6: 206.
30. Trivedi MK, Branton A, Trivedi D, Nayak G, Gangwar M, et al. (2015) Antibiofilm, biochemical reactions, and genotypic pattern of biofield treated *Pseudomonas aeruginosa*. *J Trop Dis* 4: 181.
31. Trivedi MK, Branton A, Trivedi D, Nayak G, Bairwa K, et al. (2015) Effect of biofield treatment on physical, thermal, and spectral properties of SFRE 199-1 mammalian cell culture medium. *Advances in Biochemistry* 3: 77-85.
32. Trivedi MK, Branton A, Trivedi D, Nayak G, Bairwa K, et al. (2015) Physical, thermal, and spectroscopic characterization of biofield energy treated Murashige and Skoog plant cell culture media. *Cell Biology* 3(4): 50-57.
33. Trivedi MK, Branton A, Trivedi D, Nayak G, Mondal SC, et al. (2015) Evaluation of plant growth, yield and yield attributes of biofield energy treated mustard (*Brassica juncea*) and chick pea (*Cicer arietinum*) seeds. *Agriculture, Forestry and Fisheries* 4: 291-295.
34. Trivedi MK, Branton A, Trivedi D, Nayak G, Mondal SC, et al. (2015) Morphological characterization, quality, yield and dna fingerprinting of biofield energy treated alphonso mango (*Mangifera indica L.*). *Journal of Food and Nutrition Sciences* 3: 245-250.
35. Desktop X-ray Diffractometer "MiniFlex+" (1997) *The Rigaku Journal* 14: 29-36.
36. Zhang T, Paluch K, Scalabrino G, Frankish N, Healy AM, et al. (2015) Molecular structure studies of (1S,2S)-2-benzyl-2,3-dihydro-2-(1H-inden-2-yl)-1H-inden-1-ol. *J Mol Struct* 1083: 286-299.
37. Langford JI, Wilson AJC (1978) Scherrer after sixty years: A survey and some new results in the determination of crystallite size. *J Appl Cryst* 11: 102-113.
38. Trivedi MK, Sethi KK, Panda P, Jana S (2017) A comprehensive physicochemical, thermal, and spectroscopic characterization of zinc (II) chloride using X-ray diffraction, particle size distribution, differential scanning calorimetry, thermogravimetric analysis/differential thermogravimetric analysis, ultraviolet-visible, and Fourier transform-infrared spectroscopy. *International Journal of Pharmaceutical Investigation* 7(1): 33-40.
39. Trivedi MK, Sethi KK, Panda P, Jana S (2017) Physicochemical, thermal

- and spectroscopic characterization of sodium selenate using XRD, PSD, DSC, TGA/DTG, UV-vis, and FT-IR. *Marmara Pharmaceutical Journal* 21/2: 311-318.
40. Raza K, Kumar P, Ratan S, Malik R, Arora S (2014) Polymorphism: The phenomenon affecting the performance of drugs. *SOJ Pharm Pharm Sci* 1: 10.
41. Brittain HG (2009) Polymorphism in pharmaceutical solids in *Drugs and Pharmaceutical Sciences*, volume 192, 2nd Edn, Informa Healthcare USA, Inc., New York, USA.
42. Censi R, Martino PD (2015) Polymorph impact on the bioavailability and stability of poorly soluble drugs. *Molecules* 20(10): 18759-18776.
43. Blagden N, De Matas M, Gavan PT, York P (2007) Crystal engineering of active pharmaceutical ingredients to improve solubility and dissolution rates. *Adv Drug Deliv Rev* 59(7): 617-630.
44. Chereson R (2009) Bioavailability, bioequivalence, and drug selection. In: Makoid CM, Vuchetich PJ, Banakar UV (Eds.), *Basic pharmacokinetics (1st edn)* Pharmaceutical Press, London.
45. Chereson R (2009) Bioavailability, bioequivalence, and drug selection. In: Makoid CM, Vuchetich PJ, Banakar UV (Eds.), *Basic pharmacokinetics (1st edn)* Pharmaceutical Press, London.
46. Khadka P, Ro J, Kim H, Kim I, Kim JT, et al. (2014) Pharmaceutical particle technologies: An approach to improve drug solubility, dissolution and bioavailability. *Asian J Pharm Sci* 9(6): 304-316.
47. Vora L, Sita V G, Vavia P (2017) Zero order-controlled release delivery of cholecalciferol from injectable biodegradable microsphere: *In-vitro* characterization and *in-vivo* pharmacokinetic studies. *European Journal of Pharmaceutical Sciences* 107: 78-86.
48. Zhao Z, Xie M, Li Y, Chen A, Li G, et al. (2015) Formation of curcumin nanoparticles *via* solution-enhanced dispersion by supercritical CO₂. *Int J Nanomedicine* 10: 3171-3111.



Creative Commons Attribution 4.0
International License

For possible submissions Click Here

[Submit Article](#)



Advances in Complementary & Alternative Medicine

Benefits of Publishing with us

- High-level peer review and editorial services
- Freely accessible online immediately upon publication
- Authors retain the copyright to their work
- Licensing it under a Creative Commons license
- Visibility through different online platforms